Two-step machine learning assisted extraction of VCSEL parameters

Two-step machine learning assisted extraction of VCSEL parameters

Ihtesham Khan, Muhammad Umar Masood, Lorenzo Tunesi, Enrico Ghillino, Andrea Carena, et al.

Ihtesham Khan, Muhammad Umar Masood, Lorenzo Tunesi, Enrico Ghillino, Andrea Carena, Vittorio Curri, Paolo Bardella, "Two-step machine learning assisted extraction of VCSEL parameters," Proc. SPIE 12415, Physics and Simulation of Optoelectronic Devices XXXI, 124150P (10 March 2023); doi: 10.1117/12.2650220

SPIE.

Event: SPIE OPTO, 2023, San Francisco, California, United States

Two-step Machine Learning Assisted Extraction of VCSEL parameters

Ihtesham Khan[a], Muhammad Umar Masood[a], Lorenzo Tunesi[a], Enrico Ghillino[b], Andrea Carena[a], Vittorio Curri[a], and Paolo Bardella[a]

[a]Department of Electronics and Telecommunications, Politecnico di Torino, Torino, Italy
[b]Synopsys, Inc., Ossining, NY 10562, United States

ABSTRACT

We propose a Machine Learning (ML) assisted procedure to extract Vertical Cavity Surface Emitting Lasers (VCSELs) parameters from Light-Current (L-I) and S21 curves using a two-step algorithm to ensure high accuracy of the prediction. In the first step, temperature effects are not included and a Deep Neural Network (DNN) is trained on a dataset of 10000 mean-field VCSEL simulations, obtained changing nine temperature-independent parameters. The agent is used to retrieve those parameters from experimental results at a fixed temperature. Secondly, additional nine temperature-dependent parameters are analyzed while keeping as constant the extracted ones and changing the operation temperature. In this way a second dataset of 10000 simulations is created and a new agent in trained to extract those parameters from temperature-dependent L-I and S21 curves.

Keywords: Vertical Cavity Surface Emitting Lasers, Machine Learning, Deep Learning,Parameters Extraction.

1. INTRODUCTION

VCSEL have been accurately described by a number of computationally effective models that have been developed in recent years, many of them being also available in commercial software aimed at simulating VCSEL sources as a single component or as part of larger optoelectronic systems. The complexity of these models, generally including a description of carrier and photon dynamics with temperature dependent effects, is a crucial element for accuracy of their result. Unfortunately, accurate results also need the proper setting of numerous physical parameters that must be carefully adjusted in order to faithfully represent the behavior of a real VCSEL source.

The extraction of these unidentified physical parameters from the experimental curves is typically time consuming and relies on techniques like regression analysis or trial-and-error approaches. In this work, we suggest an ML-based solution to the problem that can successfully extract the necessary VCSEL parameters from experimental data. Although for our study we consider the VCSEL model available in the Synopsys OptSim circuit simulation environment,[1] the proposed procedure can be easily adapted to extract the parameters of different VCSELs and the edge-emitting laser model.

2. VERTICAL CAVITY SURFACE EMITTING LASERS MODEL

The considered VCSEL model, which is accessible as a standard OptSim block, extends the model proposed in,[2] including the temporal evolution of the field phase.[3] In cylindrical geometry, the number of carriers is expanded

Send correspondence to Paolo Bardella. Mail: paolo.bardella@polito.it

Physics and Simulation of Optoelectronic Devices XXXI, edited by Bernd Witzigmann, Marek Osiński, Yasuhiko Arakawa, Proc. of SPIE Vol. 12415, 124150P
 · 0277-786X · doi: 10.1117/12.2650220

Parameter	Range	Value
Current injection η_i	0.4 to 1	0.8
Photons lifetime τ_p	1.5 ps to 3.5 ps	2.5 ps
Carrier lifetime τ_n	1.5 ns to 3.5 ns	2.5 ns
Gain coefficient g_0	$25\,000\,\mathrm{s}^{-1}$ to $75\,000\,\mathrm{s}^{-1}$	$50\,000\,\mathrm{s}^{-1}$
Carrier transparency number N_tr	0.5×10^6 to 1.5×10^6	1×10^6
Gain saturation factor ε	3×10^{-7} to 6×10^{-7}	5×10^{-7}
Overlap coeff. $(N_0 - S)$ γ_{00}	0.75 to 1	1
Overlap coeff. $(N_0 - S)$ γ_{01}	0.2 to 0.5	0.38
Diffusion parameter h_diff	7.5 to 22.5	15

Table 1: Parameters investigated and variation ranges for generating 1st dataset at 25 °C. Last column values were obtained from the DNN analysis and were used for the generation of the 2nd dataset.

Parameter	Range
Gain coeff. parameter $a_{\mathrm{g}0}$	-0.6 to -0.2
Gain coeff. parameter $a_{\mathrm{g}1}$	$1\times10^{-3}\,\mathrm{K}^{-1}$ to $3\times10^{-3}\,\mathrm{K}^{-1}$
Gain coeff. parameter $a_{\mathrm{g}2}$	$3\times10^{-7}\,\mathrm{K}^{-2}$ to $3\times10^{-8}\,\mathrm{K}^{-2}$
Gain coeff. parameter $b_{\mathrm{g}0}$	0.5 to 3
Gain coeff. parameter $b_{\mathrm{g}1}$	$-5\times10^{-3}\,\mathrm{K}^{-1}$ to $-2\times10^{-3}\,\mathrm{K}^{-1}$
Gain coeff. parameter $b_{\mathrm{g}2}$	$1\times10^{-5}\,\mathrm{K}^{-2}$ to $3\times10^{-5}\,\mathrm{K}^{-2}$
Transparency number param. $c_{\mathrm{n}0}$	-0.5 to -2
Transparency number param. $c_{\mathrm{n}1}$	$4\times10^{-3}\,\mathrm{K}^{-1}$ to $1.2\times10^{-2}\,\mathrm{K}^{-1}$
Transparency number param. $c_{\mathrm{n}2}$	$3\times10^{-6}\,\mathrm{K}^{-2}$ to $1.2\times10^{-5}\,\mathrm{K}^{-2}$

Table 2: Parameters investigated and variation ranges for generating the 2nd dataset.

in the Bessel series, and the first two terms, N_0 and N_1, are evaluated using[4]

$$\frac{\mathrm{d}N_0}{\mathrm{d}t} = \frac{\eta_\mathrm{i} I}{q} - \frac{N_0}{\tau_\mathrm{n}} - \frac{G\left[\gamma_{00}(N_0 - N_\mathrm{t}) - \gamma_{01}N_1\right]}{1+\varepsilon S}S - \frac{I_\mathrm{l}}{q} \tag{1}$$

$$\frac{\mathrm{d}N_1}{\mathrm{d}t} = -\frac{N_1}{\tau_\mathrm{n}}(1+h_\mathrm{diff}) + \frac{G\left[\phi_{100}(N_0 - N_\mathrm{t}) - \phi_{101}N_1\right]}{1+\varepsilon S}S \tag{2}$$

$$\frac{\mathrm{d}S}{\mathrm{d}t} = -\frac{S}{\tau_\mathrm{p}} + \frac{\beta N_0}{\tau_\mathrm{n}} + \frac{G\left[\gamma_{00}(N_0 - N_\mathrm{t}) - \gamma_{01}N_1\right]}{1+\varepsilon S} \tag{3}$$

$$\frac{\mathrm{d}\phi}{\mathrm{d}t} = \frac{\alpha}{2}\frac{G\left[\gamma_{00}(N_0 - N_\mathrm{tr}) - \gamma_{01}N_1\right]}{1+\varepsilon S} \tag{4}$$

$$G(T) = G_0\frac{a_{\mathrm{g}0} + a_{\mathrm{g}1}T + a_{\mathrm{g}2}T^2}{b_{\mathrm{g}0} + b_{\mathrm{g}1}T + b_{\mathrm{g}2}T^2} \tag{5}$$

$$N_\mathrm{t}(T) = N_\mathrm{tr}\left(c_{\mathrm{n}0} + c_{\mathrm{n}1}T + c_{\mathrm{n}2}T^2\right) \tag{6}$$

Equations (1-6) describe then the temporal evolution of the carriers N_0 and N_1, the photons number S and the phase ϕ in a mean field approximation. In Eqs. (1-4), I is the injected current, q is the electron charge, I_l is the leakage current, ϕ_{100} and ϕ_{101} are the overlap coefficient between the expanded carrier terms and the optical field, β is the spontaneous emission coefficient, and α is the linewidth enhancement factor. With the fitting parameters indicated in Eq.s (5-6),[2] a phenomenological representation of the gain G and the carrier transparency number N_t is introduced to model the temperature T dependency of the VCSEL behavior. Additional parameters defined in Eq.s (1-6), the objective of the ML study, are defined in Tables 1 and 2.

3. RESULTS AND CONCLUSION

The extraction of the 18 parameters given in Tables 1 and 2 is the main goal of the our analysis. Executing the study in two steps reduces its complexity and requires the training of two smaller ML agents, mostly using a DNN architecture with three hidden layers and 10 neurons per layer.[5] ReLU served as the activation function

and Mean Square Error (MSE) served as the loss function in the proposed DNN model. The DNN model is set up for 100 training steps with 0.01 as the default learning rate. The percentages of the training and test sets are 70% and 30%, respectively, of the entire dataset.

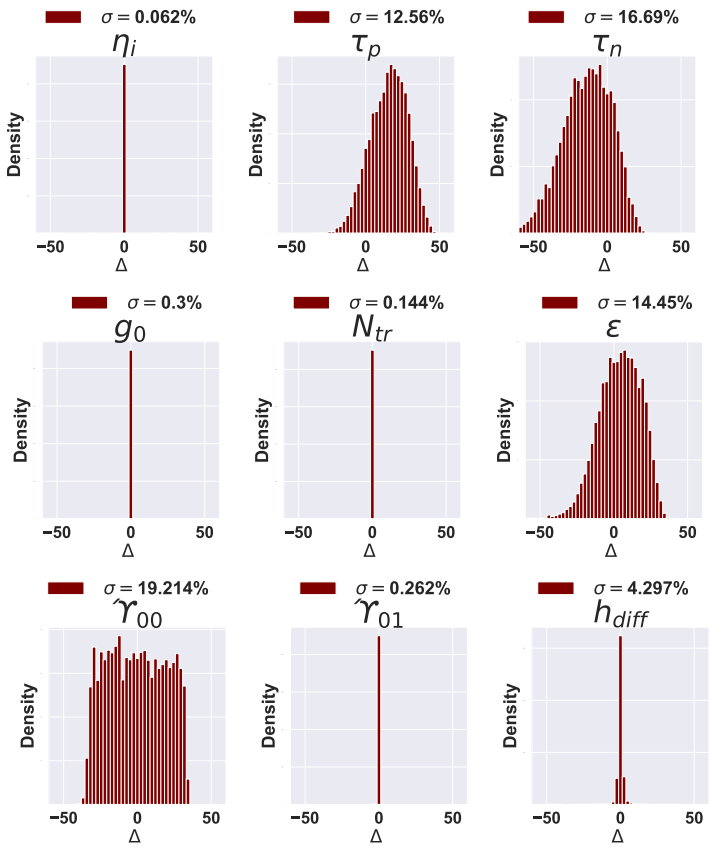

Figure 1: Relative prediction error of 1st agent for the nine considered parameters.

The initial DNN agent is used to extract the parameters listed in Table 1 and is trained on the data obtained at a constant temperature. The parameters appearing in Table 1 are changed to their central values of the suggested ranges, while all other parameters are left at their default values, as indicated in OptSim. In specific, a dataset of 10 000 simulations is created at the constant temperature of 25 °C, changing the values of the parameters listed in Table 1 and keeping all other parameters fixed. The dataset contains 16 instances of the L-I curve for each set of parameters, generated for linearly spaced injected currents I in the 1 mA to 25 mA. Furthermore, responses to small-signal modulation responses are calculated at 6 mA, 12 mA, 18 mA, and 24 mA; for each curve, 16 samples are recorded, at frequencies that are logarithmically spaced between 10 kHz and 50 GHz. The relative predicted errors for the nine parameters considered by this agent are presented in Fig 1; the most critical parameter is γ_{00}, with a relative error of approximately 20%, while for η_i, g_0, γ_{01}, and h_{diff} the relative error is well below 10%.

The trained agent is used to extract the randomly generated parameters used in an additional set of simulations used as reference; the extracted values, listed in the last column of Table 1, are kept constant in the second analysis. In a real-case scenario, this additional data would be obtained from experimental measurements. The second DNN agent is trained using L-I curves calculated at different temperatures changing the parameters listed in Table 2 all of which introduce a dependence of gain and transparency carrier number with temperature. The best values for those parameters can subsequently be determined using the experimentally collected data by a second ML agent. For the second study, a new dataset of 10 000 simulations is created. It contains data from four L-I curves derived at 10 °C, 25 °C, 40 °C, and 55 °C and corresponding S21 curves; the relative predicted errors for the nine parameters considered by this agent are presented in Fig 2. While the relative errors are between

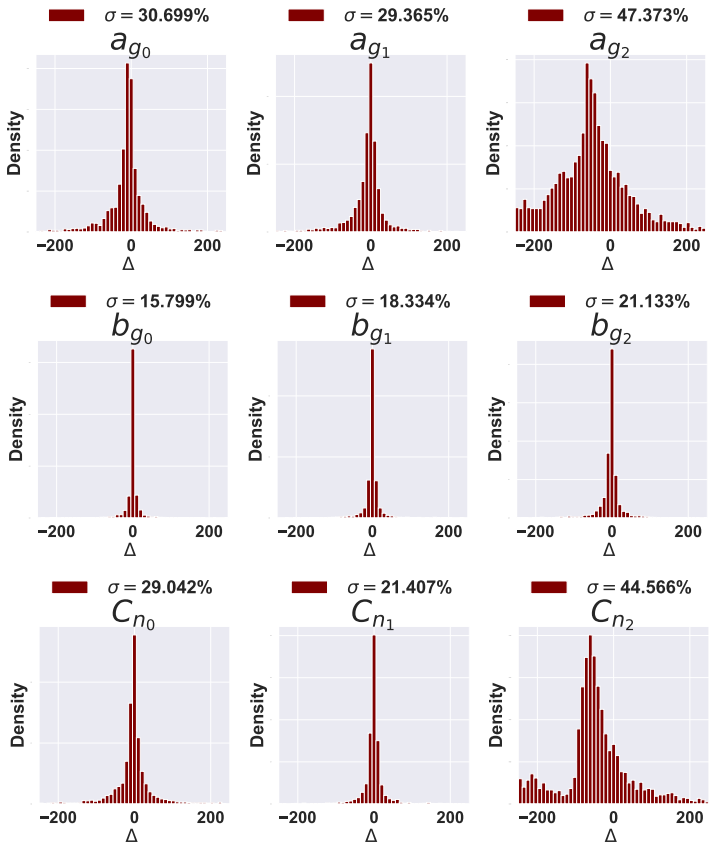

Figure 2: Relative prediction error of 2nd agent for the nine considered parameters.

18% and 47%, the set of values extracted from the first and second agents allows one to obtain an excellent approximation of the L-I and S21 curves of the reference case.

4. CONCLUSION

We described a DNN based assisted procedure to extract fundamental VCSELs parameters from L-I and S21 curves. The two-step procedure focuses first on the extraction of temperature-independent parameters and then on the determination of the temperature dependent ones. The proposed approach can also be applied to edge-emitting lasers without significant changes.

REFERENCES

[1] https://www.synopsys.com/photonic-solutions/pic-design-suite.html.

[2] Mena, P. et al., "A comprehensive circuit-level model of vertical-cavity surface-emitting lasers," *JLT* **17**(12), 2612–2632 (1999).

[3] Jungo, M. et al., "Vistas: a comprehensive system-oriented spatiotemporal vcsel model," *IEEE JSTQE* **9**(3), 939–948 (2003).

[4] Mena, P. et al., "Compact representations of mode overlap for circuit-level vcsel models," in [*IEEE LEOS 2000*], **1**, 234–235 vol.1 (2000).

[5] Khan, I. et al., "Machine-learning-aided abstraction of photonic integrated circuits in software-defined optical transport," in [*Next-Generation Optical Communication: Components, Sub-Systems, and Systems X*], **11713**, 145–150, SPIE (2021).